Gilbert cell down-conversion mixer for THz wireless communication with passive baluns

Abdeladim El Krouk[1], Abdelhafid Es-Saqy[2], Mohammed Fattah[1], Said Mazer[2], Mahmoud Mehdi[3], Moulhime El Bekkali[2], Catherine Algani[4]

[1]IMAGE Laboratory, Faculty of Sciences, Moulay Ismail University, Meknes, Morocco
[2]Artificial Intelligence, Data Sciences and Emerging Systems Laboratory, Sidi Mohamed Ben Abdellah University, Morocco
[3]Microwaves Laboratory, Faculty of Sciences and Fine Arts, CRITC, AUL University, Beirut, Lebanon
[4]ESYCOM Laboratory, Gustave Eiffel University, CNRS, Le Cnam, Paris, France

## Article Info

ABSTRACT

This article presents the design of an active down-conversion mixer for the superheterodyne receiver system for 6G wireless communications. This mixer is developed based on the Gilbert cell in the terahertz frequency band, using the $PH15$ transistor from United Monolithic Semiconductors (UMS) Foundry in monolithic microwave integrated circuit (MMIC) technology. We used the charge injection method to increase our mixer's conversion gain. In addition, we integrated a buffer stage at the mixer outputs to facilitate impedance matching and improve linearity. The power dividers used in this chapter are based on transmission lines from Agilent's advanced design system (ADS) tool, connected to the input and output ports of the circuit. The proposed architecture offers a high conversion gain of 15.2 dB, with a low local oscillator (LO) power of 0 dBm, a low double sideband (DSB) noise figure (NF) of around 7.1 dB, a 1 dB compression point of -16 dBm, and good radio frequency $(RF) - LO$ port isolation of 63.2 dB, at a RF of 0.14 THz.
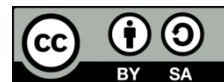
Corresponding Author:

Abdeladim El Krouk
IMAGE Laboratory, Faculty of Sciences, Moulay Ismail University
Meknes, Morocco
Email: abdeladim.elkrouk@usmba.ac.ma

1. INTRODUCTION

Wireless communications technology is moving towards higher operating frequencies, i.e., from 0.1 to 3 THz [1], [2]. These frequency bands are envisaged for the next generation of wireless networks 6G [3]. This evolution is necessary to achieve even higher data rates and reduced latency compared to current networks. To satisfy the demands of a growing number of new applications such as autonomous driving, robotic control, the internet of things (IoT) and THz localization/navigation [4], [5].

A high bandwidth characterizes the terahertz frequency band. It enables a large amount of data to be transmitted at higher speeds, up to several gigabits per second [2]. These frequency bands hold great promise for the future generation of wireless communication systems. Their very short wavelengths make it possible to manufacture high-gain, antennas while maintaining tiny physical dimensions and privileged confidentiality of communications [6]. In addition, the THz frequency band offers several advantages in different fields, such as security controls, concealed weapons detection, medical imaging, safety [7].

In particular, the frequency band around 0.14 THz is exciting, as it is characterized by low atmospheric attenuation (1 dB/km) and localized between two molecular absorption peaks at 119 GHz and 183 GHz [8], [9]. The significance of atmospheric absorption effects at high frequencies has been acknowledged on numerous

occasions [10]. As the wavelength gets closer to the dimensions of particles like snow, dust, and rain, the significance of scattering effects becomes more pronounced [6].

For these reasons, many downconverters have been presented near this band [10]-[13]. A double-balanced downconverter mixer, based on Gilbert's culling, designed explicitly for frequency modulated continuous-wave (FMCW) radar implementation, was introduced in [14]. Kavivarman *et al.* [15] present a comparative study of the different methods used to improve the different performances of the Gilbert mixer. The demonstration of a down-conversion mixer operating from 60 to 113 GHz in 90 nm CMOS technology is presented in [16]. In addition, The design of a wideband intermediate frequency (IF) receiver operating between 110 and 140 GHz, used in 65 nm CMOS technology, as reported in [17].

The major difficulties in current THz communications lie in the complexity of modulation and demodulation methods, as well as in the high atmospheric extinction. In particular, the design of a frequency down-conversion mixer over 100 GHz is complex due to criteria concerning conversion gain, passband, noise figure (NF) and linearity. Consequently, we have proposed a Gilbert cell-based downconverting mixer, using the charge injection technique and two power dividers, operating at the 140 GHz frequency band for a superheterodyne receiving chain, as shown in Figure 1. The radio frequency (RF) receiver generally consists of an antenna to capture the received signal [18]. Following this, there is a low-noise amplifier (LNA) that amplifies the RF-filtered signal. Lastly, the down-converting mixer plays an essential role within the RF receiver by enabling the conversion of the RF to a lower IF, achieved through the utilization of a local oscillator (LO) signal [19], [20]. The organization of this paper is outlined as: in the second section, we have presented the proposed mixer circuit and the design and simulations of the passive baluns. In the third section, we analyze the simulation results of the Gilbert mixer with integrated baluns. Finally, the last section presents the circuit layout and simulation.
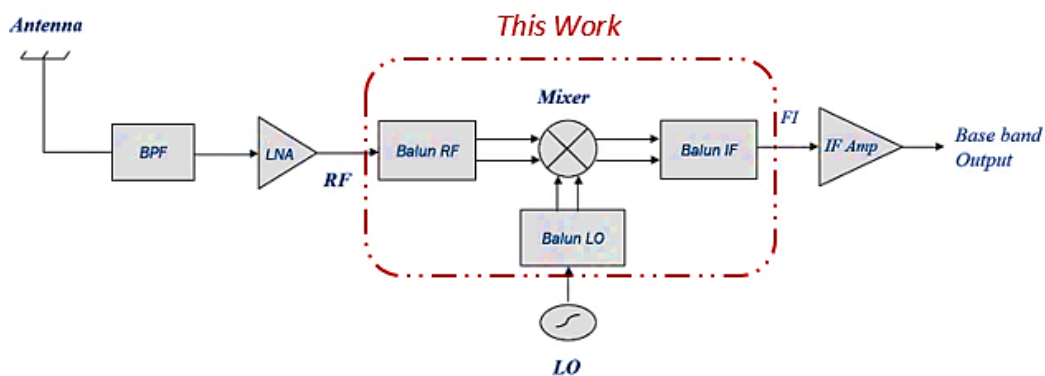

Figure 1. The architecture of a superheterodyne receiver

2. CIRCUIT DESIGN
2.1. Electrical circuit diagram

The mixer suggested in this article is essentially founded on the double-balanced Gilbert cell. This structure reduces even-order distortion and ensures good isolation between ports. It is an active mixer used in the architecture of a superheterodyne receiver. It converts the RF frequency of 0.14 THz to the IF of 1 GHz using a LO signal fixed at 0.139 THz. The circuit is designed using the 0.15 μm pHEMT transistor of the PH15 process in monolithic microwave integrated circuit (MMIC) technology.

The electrical circuit diagram is depicted in Figure 2, consisting of three primary stages. Firstly, there is a differential transconductance stage that includes a differential pair composed of transistors M1 and M2, each having a width of 54 μm. These two transistors operate in saturation mode, facilitating the conversion of the RF input voltage into a differential current. Subsequently, the switching stage represents the core of the circuit. It comprises two differential pairs consisting of transistors M3-M6, which operate close to the pinch-off region with a width of 43 μm. This enables the multiplication of the RF signal with the LO signal. And a load stage consists of two 880 Ω resistors (R1 and R2). Its role is to convert the current from the switching stage into the IF output voltage.

We use the charge injection technique, based on minimum noise to determine the optimal width of the RF transistors [21], [22]. The principle of this technique is to boost the current in the RF stage by inserting two 143 Ω resistors (R3 and R4) to inject current into transistors M1 and M2. This technique aims to increase the conversion gain, which is represented by the relationship (1):

$$G_c = \frac{2}{\pi} \times g_m \times R_L \qquad (1)$$

G_c is the conversion gain, g_m represents the transconductance, while R_L denotes the load resistance of the circuit.
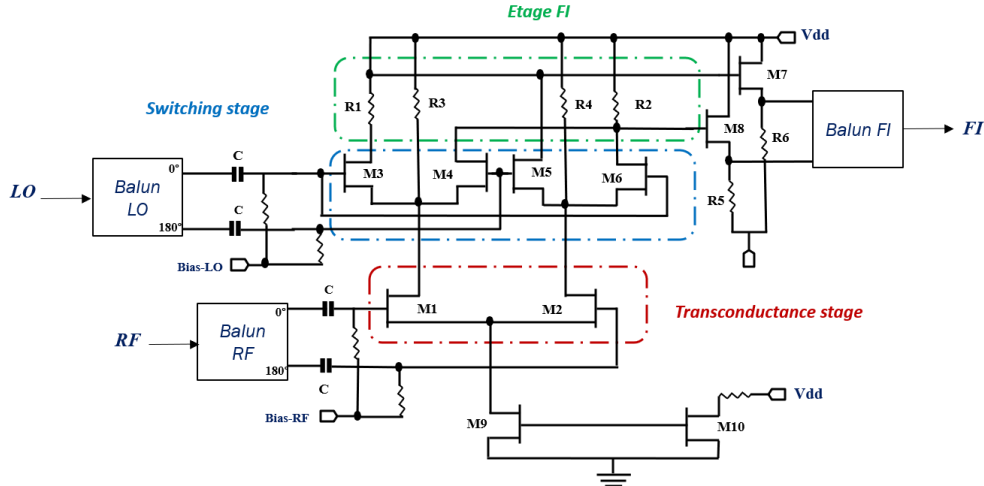

Figure 2 Topology of the proposed mixer

We integrate two buffer stages at the output of our proposed circuit, consisting of common-source transistors M7 and M8, each with four fingers (n=4) and a total width of 40 μm (4×40 μm), in order to match the output and increase the conversion gain of the proposed circuit. And a current mirror consisting of two transistors, M9 and M10, with a width of 70 μm and 42 μm, respectively, are used to supply additional current to the circuit's amplifier stage. So, to get the best possible result, it's necessary to strike an appropriate balance between the following parameters: isolation, conversion gain, LO power, linearity, and NF.

2.2. Baluns
2.2.1. Balun radio frequency/local oscillator

The Figure 3 illustrates the design of the passive RF/LO, balun manufactured using transmission lines and the resistive network from the united monolithic semiconductors (UMS) foundry to increase bandwidth [23]. The balun is composed of a single input port and two output ports, and it transforms the RF/LO signal into two signals of identical amplitude, phased 180 degrees apart. Figure 4 illustrates the frequency-dependent variation in phase difference between the two RF balun output ports. We can see that the circuit's two output ports have a phase difference of 180 degrees at 140 GHz.
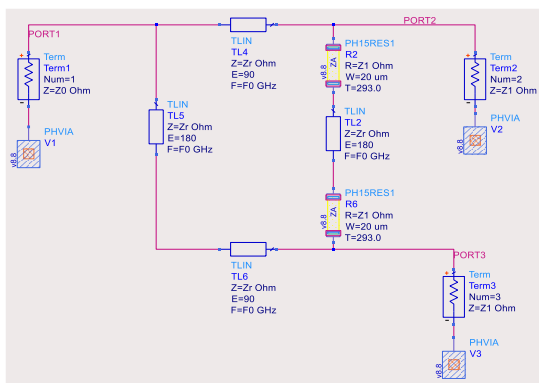

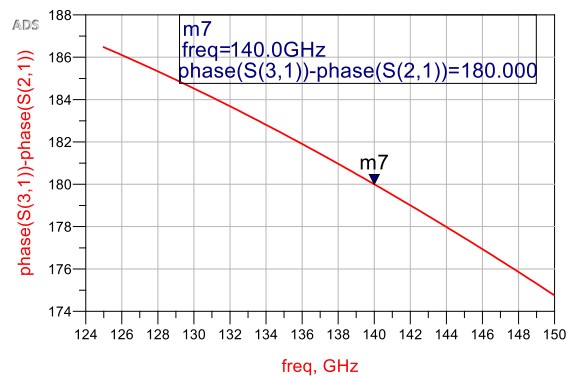Figure 3. Advanced design system (ADS) diagram of a passive balun

Figure 4. The variation in phase difference at the frequency of 140 GHz

Figure 5 shows that S21 and S31 have the same value (-3.020 dB) at 140 GHz, indicating that power division in ports 2 and 3 is achieved. The variation of the balun's amplitude difference is shown in Figure 6, where it is observed that the amplitude difference between the two output ports is approximately zero (0.013 dB) which corresponds approximately to the same amplitude.
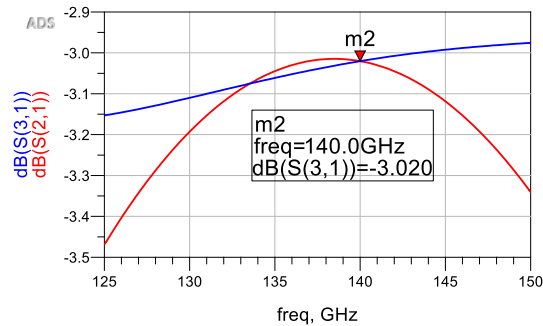

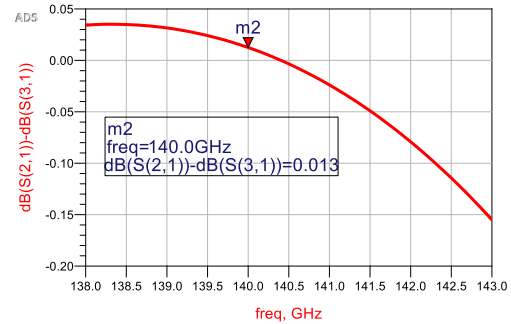Figure 5. Parameters S21 and S31 plotted against frequency in GHz

Figure 6. Amplitude difference as a function of frequency in GHz

2.2.2. Balun IF

We operate the balun circuit (RF/LO) in coupler mode on the mixer output ports (IF1, IF2). The coupler consists of two input ports, IF1, IF2, 180 degrees out of phase, and an IF output port of the same amplitude, operating at 1 GHz. As shown in Figures 7 and 8, parameters S21 and S31 are used to evaluate the phase and amplitude difference of the balun ports. The simulation results show a phase shift of 180 degrees between ports (IF1, IF) and (IF1, IF2) at 1 GHz. And an amplitude difference between the two ports of 0.38 dB, approximately zero. So, the simulation results give good balun performance at 1 GHz.
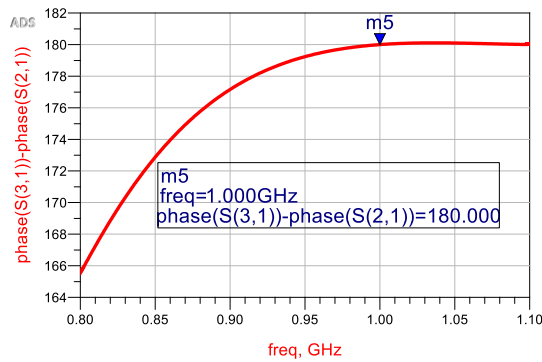

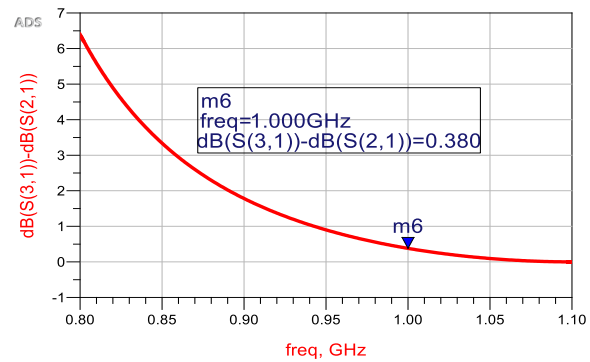Figure 7. Variation in the phase difference of the output ports at the frequency of 1 GHz

Figure 8. The amplitude difference of the output ports as a function of frequency

3. MIXER SIMULATION RESULTS
3.1. Radio frequency and local oscillator power

Figure 9 displays the change in conversion gain relative to the LO input power. The conversion gain peaks at 15.249 dB with the LO injected power set to 0 dBm. NF in double sideband (DSB) observed is approximately 7.15 dB at an LO input power of 0 dBm, as illustrated in Figure 10.

Figure 11 illustrates the conversion gain versus RF power injected curve. It can be observed that the C_G achieves a maximum value of 15.249 dB for the RF input power of -25 dBm. So, the optimum values of LO and RF powers are 0 dBm and -25 dBm, respectively. These optimum values ensure an excellent conversion gain and a low NF. So, we use these optimum LO and RF power values for all future simulations.
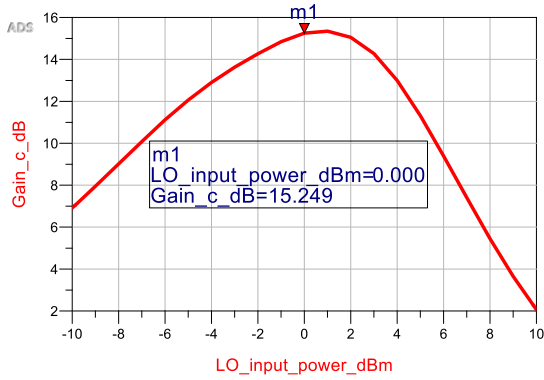
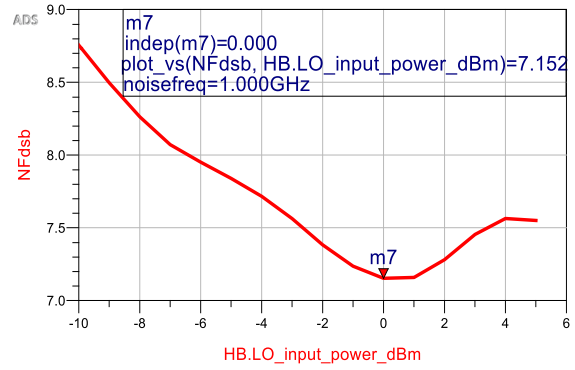Figure 9. The variation of C_G in dB as a function LO_input_pwr
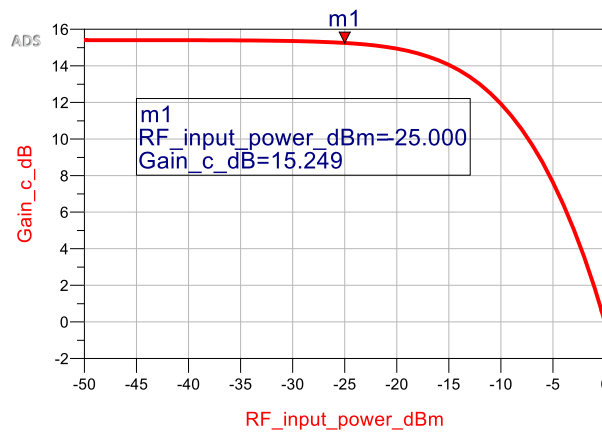

Figure 10. DSB NF of the mixer

Figure 11. The curve of C_G versus RF_input_ power_dBm

3.2. Mixer linearity

The P1dB and the third-order intercept point (IIP3) are considered the most commonly used parameters to evaluate the linearity of the mixers. Figure 12 shows the variation of IF output power versus radio-frequency power injected at input. We observe that the value of the 1 dB compression point, at which the conversion gain is reduced by 1 dB, is -16 dBm.

In addition, the IIP3 was achieved when applying two frequency signals, F_RF1 and F_RF2, to the RF access, which are 140.002 GHz and 139.998 GHz, respectively. Figure 13 shows the fundamental output power and third-order intermodulation versus injected power RF. We can deduce that the IIP3 is -6.04 dBm. This demonstrates that our proposed mixer has good linearity.
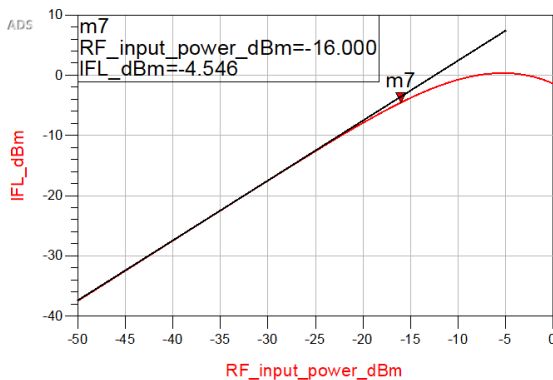

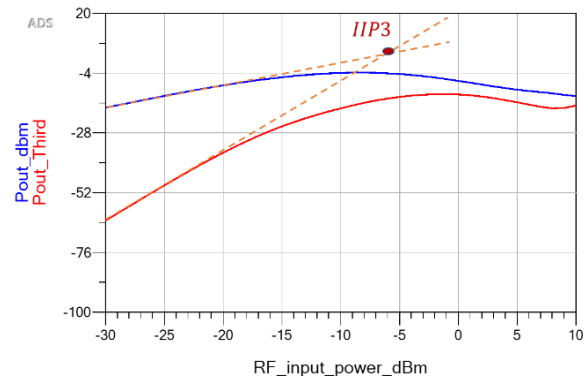Figure 12. The P1dB value of the mixer

Figure 13. The IIP3

3.3. Port-to-port isolation

The curve in Figure 14 shows the evolution of isolation between the three ports of the circuit changes with varying LO power. In the down-conversion mixer, isolation between LO_RF ports is essential, reflecting the circuit's ability to avoid LO signal leakage on the RF access. This mixer achieves good LO_RF isolation of 63.21 dB at LO power levels of 0 dBm. The isolations between RF_IF and LO_IF ports are more than 100 dB.
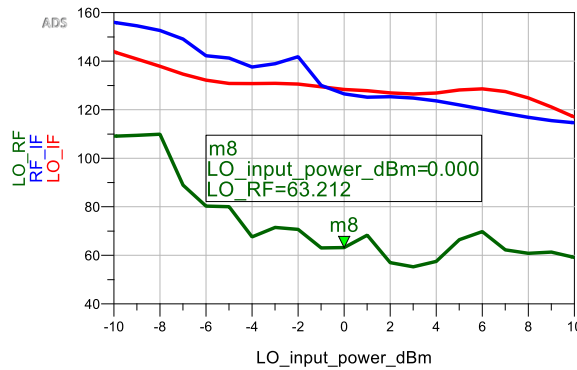

Figure 14. The evolution of isolation between LO_RF, RF_IF, and LO_IF ports as a versus LO power

4. LAYOUT DESIGN OF THE CIRCUIT

The layout schematic of the proposed Gilbert cell mixer is depicted in Figure 15. The layout consists of three parts: the mixer itself, along with three access pads for RF, LO, and IF, and three polarization pads. Together, these components enable the design of a mixer for down-conversion in the 140 GHz frequency band, while also facilitating the rejection of unwanted output signals. The circuit as a whole has a total surface area of 4.75 mm², with dimensions of 2.5 mm long by 1.9 mm wide. It is implemented on a GaAs substrate of PH15 technology from the UMS foundry.
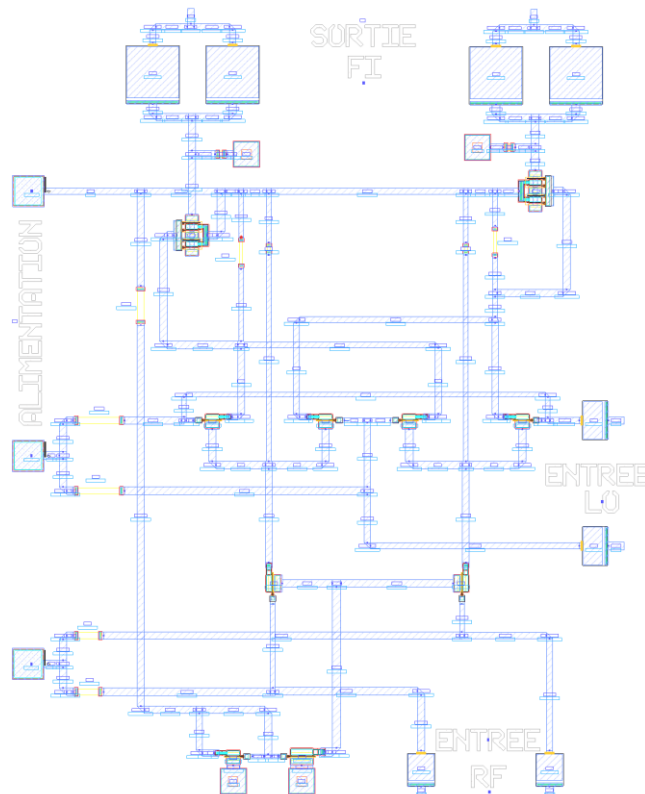

Figure 15. Gilbert cell mixer circuit layout

Figures 16-18 show the post-layout simulation results of the conversion gain, the DSB NF, and the linearity, respectively. The conversion gain of the proposed circuit attains a maximum value of -6.16 dB for a LO power of 10 dBm and -14.74 dB for a LO power of 2 dBm, is shown in Figure 16. The simulation of the NF at DSB, as a function of LO power, is illustrated in Figure 17. It exhibits a low NF of around 20 dB for an LO power of 10 dBm. Additionally, the 1 dB compression point is determined based on the variation in IF output power relative to the RF input power, as shown in Figure 18. It also demonstrates excellent linearity, approximately 6 dB.
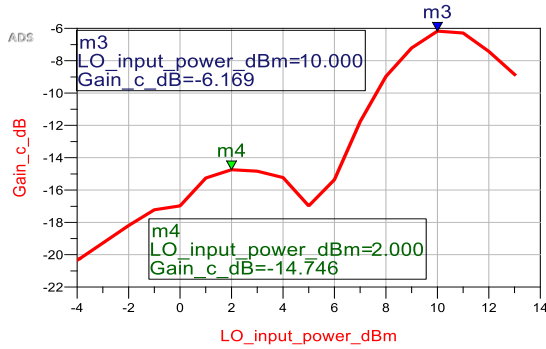

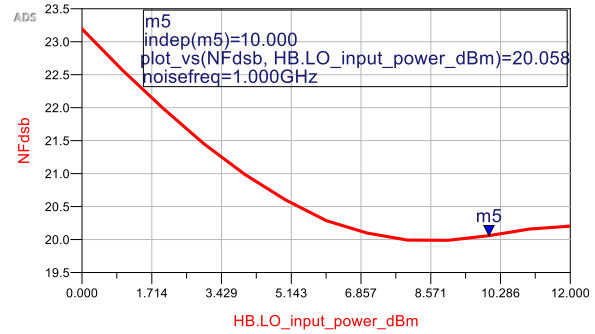Figure 16. Evolution of C_G as a function of LO_input_power_dBm

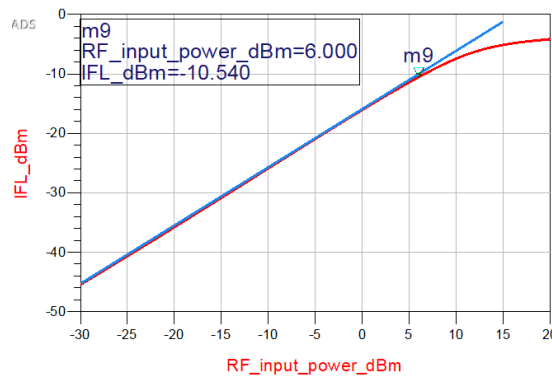Figure 17. The variation of the DSB NF of the mixer as a function of (HB. LO_input_power)

Figure 18. The P1dB value of the mixer

The various performances of the proposed mixer are presented in Table 1 and compared with those of other recently published millimeter-wave mixers. Our down-converter mixer with integrated baluns performs better regarding LO-RF isolation, NF, and linearity. It features good conversion gain and the ability to operate with low LO signal power. In addition, the NF noise of the mixer proposed in this article is lower than that of the structures studied in [24], [25].

Table 1. Summary of mixer performance and comparison with other mixers

Ref.	Circuit topology	RF-freq. (GHz)	CG (dB)	LO power (dBm)	NF (dB)	LO-RF iso. (dB)	1-dB compression point (dBm)	IIP3 (dBm)
[7]	Gilbert-cell mixer	128-160	−6	0	-	-	-15	-
[10]	Mixer double-balanced	140-170	11	0	<15	-	−13	-
[15]	90 nm	60-113	18	3.2	17.1	43.1	-	5.1
[17]	65-nm CMOS	110-140	7	-	14	-	-21	-
[26]	Gilbert-cell mixe	120-140	10-8.2	-	-	>40	-	-
[27]	CCPT-RL-based IF load	88-100	14.6	1	14.2	35.3	−13	1
[28]	90 nm	28	−2.14	1	14.32	> 57	−13	
This work	Double-balanced gilbert-cell	140	15.2	0	7.1	63	-16	-1.75

5. CONCLUSION

This article introduces a double-balanced mixer utilizing the Gilbert cell, built with the 0.15 µm PH15 transistor. The down-conversion mixer with passive baluns integrated into the RF and LO input ports at 0.14 THz frequency band. It offers an excellent conversion gain of 15.2 dB, an NF of 7.1 dB, and LO-RF isolation of over 63 dB. It also boasts good linearity. This mixer offers one of the most outstanding results among down-conversion mixers, with an approximate operating frequency of 0.140 THz, even with a low LO input power of 0 dBm."

REFERENCES

[1] T. S. Rappaport *et al.*, "Wireless Communications and Applications Above 100 GHz: Opportunities and Challenges for 6G and Beyond," in *IEEE Access*, vol. 7, pp. 78729-78757, 2019, doi: 10.1109/ACCESS.2019.2921522.

[2] I. F. Akyildiz, J. M. Jornet, and C. Han, "Terahertz band: Next frontier for wireless communications," *Physical Communication*, vol. 12, pp. 16-32, Sep. 2014, doi: 10.1016/j.phycom.2014.01.006.

[3] P. R. Vazquez, "6G Wireless Communication Links Operating at Frequencies beyond 200 GHz: an Analysis of their Performance and Main Limitations," Ph.D. dissertation, School of Electrical, Information and Media Engineering, University of Wuppertal, Germany, pp. 1-148, February 2021, doi: 10.25926/TVMC-Z778.

[4] A.-A. A. Boulogeorgos *et al.*, "Terahertz Technologies to Deliver Optical Network Quality of Experience in Wireless Systems Beyond 5G," in *IEEE Communications Magazine*, vol. 56, no. 6, pp. 144-151, June 2018, doi: 10.1109/MCOM.2018.1700890.

[5] T. S. Rappaport, Y. Xing, G. R. MacCartney, A. F. Molisch, E. Mellios, and J. Zhang, "Overview of Millimeter Wave Communications for Fifth-Generation (5G) Wireless Networks—With a Focus on Propagation Models," in *IEEE Transactions on Antennas and Propagation*, vol. 65, no. 12, pp. 6213-6230, Dec. 2017, doi: 10.1109/TAP.2017.2734243.

[6] J. F. Harvey, M. B. Steer, and T. S. Rappaport, "Exploiting High Millimeter Wave Bands for Military Communications, Applications, and Design," in *IEEE Access*, vol. 7, pp. 52350-52359, 2019, doi: 10.1109/ACCESS.2019.2911675.

[7] J. Yu *et al.*, "Transformer matched gilbert mixer with active balun for D band transmitter," *Microwave and Optical Technology Letters*, vol. 62, no 8, pp. 2696-2702, 2020, doi: 10.1002/mop.32219.

[8] D. Yoon, K. Song, M. Kaynak, B. Tillack, and J.-S. Rieh, "An Oscillator and a Mixer for 140-GHz Heterodyne Receiver Front-End based on SiGe HBT Technology," *Journal of Semiconductor Technology and Science (JSTS)*, vol. 15, no 1, 2015, pp. 29-34, doi: 10.5573/JSTS.2015.15.1.029.

[9] Y. Otsuki, D. Yamazaki, N. N. M. Khanh, and T. Iizuka, "A 140 GHz area-and-power-efficient VCO using frequency doubler in 65 nm CMOS," *IEICE Electronics Express*, vol. 16, no 6, 2019, pp. 1-5, doi: 10.1587/elex.16.20190051.

[10] J. Ma, J. Adelberg, R. Shrestha, L. Moeller, and D. M. Mittleman, "The Effect of Snow on a Terahertz Wireless Data Link," *Journal of Infrared, Millimeter, and Terahertz Waves*, vol. 39, no 6, pp. 505-508, 2018, doi: 10.1007/s10762-018-0486-2.

[11] F. Ahmed, M. Furqan, B. Heinemann, and A. Stelzer, "A SiGe-based broadband 140–170-GHz downconverter for high resolution FMCW radar applications," *2016 IEEE MTT-S International Conference on Microwaves for Intelligent Mobility (ICMIM)*, San Diego, CA, USA, 2016, pp. 1-4, doi: 10.1109/ICMIM.2016.7533917.

[12] B. Sene, D. Reiter, H. Knapp, H. Li, T. Braun, and N. Pohl, "An Automotive D-Band FMCW Radar Sensor Based on a SiGe-Transceiver MMIC," in *IEEE Microwave and Wireless Components Letters*, vol. 32, no. 3, pp. 194-197, March 2022, doi: 10.1109/LMWC.2021.3121656.

[13] B. Khamaisi and E. Socher, "130-320-GHz CMOS Harmonic Down-Converters Around and Above the Cutoff Frequency," in *IEEE Transactions on Microwave Theory and Techniques*, vol. 63, no. 7, pp. 2275-2288, July 2015, doi: 10.1109/TMTT.2015.2431671.

[14] M. Ravikumar and U. Eranna, "Low Power FMCW Transceiver Design With 140-ghz in CMOS 45nm Technology," *2020 IEEE International Conference for Innovation in Technology (INOCON)*, Bangluru, India, 2020, pp. 1-6, doi: 10.1109/INOCON50539.2020.9298342.

[15] J. Kavivarman, B. Partibane, and V. Vaithianathan, "Design of an Improved Gilbert Mixer for 5G Applications Using 45nm CMOS Technology," *2020 5th International Conference on Communication and Electronics Systems (ICCES)*, Coimbatore, India, 2020, pp. 33-39, doi: 10.1109/ICCES48766.2020.9137988.

[16] Y.-S. Lin and K.-S. Lan, "Design and implementation of a 60–113 GHz down-conversion mixer in 90 nm CMOS," *Analog Integrated Circuits and Signal Processing*, vol. 104, no 2, pp. 109-119, 2020, doi: 10.1007/s10470-020-01654-5.

[17] Y. Chen *et al.*, "110–140-GHz Wide-IF-Band 65-nm CMOS Receiver Design for Fusion Plasma Diagnostics," in *IEEE Microwave and Wireless Components Letters*, vol. 32, no. 6, pp. 631-634, June 2022, doi: 10.1109/LMWC.2021.3139628.

[18] S.-E. Didi, I. Halkhams, M. Fattah, Y. Balboul, S. Mazer, and M. E. Bekkali, "Design of a microstrip antenna patch with a rectangular slot for 5G applications operating at 28 GHz," *TELKOMNIKA Telecommunication, Computing, Electronics and Control*, vol. 20, no 3, pp. 527-536, 2022, doi: 10.12928/telkomnika.v20i3.23159.

[19] A. Es-Saqy *et al.*, "Very Low Phase Noise Voltage Controlled Oscillator for 5G mm-wave Communication Systems," *2020 1st International Conference on Innovative Research in Applied Science, Engineering and Technology (IRASET)*, Meknes, Morocco, pp. 1-4, 2020, doi: 10.1109/IRASET48871.2020.9092005.

[20] A. Es-Saqy *et al.*, "A 5G mm-wave compact voltage-controlled oscillator in 0.25 µm pHEMT technology," *International Journal of Electrical and Computer Engineering (IJECE)*, vol. 11, no 2, pp. 1036-1042, 2021, doi: 10.11591/ijece.v11i2.pp1036-1042.

[21] F. M. Mahmoud and M. A. Abdelghany, "Low flicker-noise RF CMOS gilbert-cell mixer for 2.4GHz wireless communication systems," *2016 International Conference on Electrical, Electronics, and Optimization Techniques (ICEEOT)*, Chennai, India, pp. 1158-1161, 2016, doi: 10.1109/ICEEOT.2016.7754866.

[22] A. El Krouk, A. Es-Saqy, M. Fattah, S. Mazer, M. El Bekkali, and M. Mehdi., "Gilbert Cell Down-Conversion Mixer for THz Wireless Communication" in *Artificial Intelligence and Smart Environment*, vol. 635, pp. 475-480, 2023, doi: 10.1007/978-3-031-26254-8_68.

[23] U. Musa, S. Babani, and A. S. Ali, "Design and simulation of 2 section microstrip Wilkinson power divider," *Bayero University Journal of Engineering and Technology (BJET)*, vol.14, no.1, pp.17-23, 2019.

[24] Z. Khan and S. Kumar, "A Next-generation down conversion mixer design using Schottky diode to improve performance for WSN," *International Journal of Computing and Digital Systems*, vol. 14, no 1, p. 10309-10316, 2023, doi: 10.12785/ijcds/1401103.

[25] M. Mohammadi and M. Yargholi, "A 29.5 GHz High gain Down-Conversion CMOS Mixer for 5G applications," *National Conférence on Electrical and Electronecs Industry*, 22 August 2021.

[26] D. Hou, W. Hong, J. Chen, P. Yan, and Y. Xiong, "A compact D-band I/Q mixer with improved transformer balun," *Microwave and Optical Technology Letters*, vol. 59, no 11, p. 2840-2844, 2017, doi: 10.1002/mop.30840.

[27] Y. -S. Lin and Y. E. Wang, "Design and Analysis of a 94-GHz CMOS Down-Conversion Mixer With CCPT-RL-Based IF Load," in *IEEE Transactions on Circuits and Systems I: Regular Papers*, vol. 66, no. 8, pp. 3148-3161, Aug. 2019, doi: 10.1109/TCSI.2019.2910223.

[28] Y. -T. Chang and K. -Y. Lin, "A 28-GHz Bidirectional Active Gilbert-Cell Mixer in 90-nm CMOS," in *IEEE Microwave and Wireless Components Letters*, vol. 31, no. 5, pp. 473-476, May 2021, doi: 10.1109/LMWC.2021.3061658.

BIOGRAPHIES OF AUTHORS

Abdeladim El Krouk 🆔 👤 SC ⟳ was born in TISSA, Morocco, in January 1991. Received his Master degree in Microelectronics from Faculty of Sciences Dhar EL Mahraz Fez Morocco, in 2016. He is now Ph.D. student in Artificial Intelligence, IMAGE Laboratory at the University of Moulay Ismail Meknes. His main research interest includes mixers and balun. He can be contacted at email: abdeladim.elkrouk@usmba.ac.ma.

Abdelhafid Es-Saqy 🆔 👤 SC ⟳ was born in TISSA, Morocco, in January 1992. Received his Master's degree in Microelectronics from Faculty of Sciences Dhar EL Mahraz Fez Morocco, in 2018. He is now Ph.D. student in Artificial Intelligence, Data Sciences and Emerging Systems Laboratory at the University of Sidi Mohamed Ben Abdellah Fez. He can be contacted at email: abdelhafid.essaqy@usmba.ac.ma.

Mohammed Fattah 🆔 👤 SC ⟳ received his Ph.D. in Telecommunications and CEM at the University of Sidi Mohamed Ben Abdellah (USMBA) Fez, Morocco, 2011. He is a professor in the Electrical Engineering Department of the High school of technology at the Moulay Ismail University (UMI), Meknes, Morocco and he is a responsible of the research team 'Intelligent Systems, Networks and Telecommunications', IMAGE laboratory, UMI. He can be contacted at email: m.fattah@umi.ac.ma.

Said Mazer 🆔 👤 SC ⟳ born in 1978. He received the Ph.D. degree in Electronics and Signal Processing from the University of Marne-La-Vallée, Champs-surMarne, France. He is currently a Full Professor with the National School of Applied Sciences of Fez, Morocco. He is membre of IASSE Laboratory, University of Sidi Mohamed Ben Abdellah Fez. His research interests include the development of microwave-photonics devices for radio-over fibre and wireless applications, and he is also involved in network security. He can be contacted at email: said.mazer@usmba.ac.ma.

Mahmoud Mehdi 🆔 📇 SC ↻ was born in Beirut, Lebanon, in 1974. He received his Ph.D. in High Frequency Communication Systems from the University of Paris Marne la Vallée, France 2005. He is an Associate Professor in the Physics Department of the Faculty of sciences at the Lebanese University, Beirut, Lebanon. His research interests include MMIC, micro-electro-mechanical systems (MEMS), radiofrequency, double balanced and distributed mixers, local oscillator, TW amplifiers, optoelectronic mixer for LIDAR system, optical systems and design, and photo-detectors. He is course leader in microwave devices for the Masters program in Electronics. He can be contacted at email: mahmoud.mehdi@ul.edu.lb.

Moulhime El Bekkali 🆔 📇 SC ↻ holder of a doctorate in 1991 from the USTL University Lille 1 France, he worked on antennas printed in X-band and their applications to microwave radar. Since 1992, he was a Professor at the Graduate School of Technology, Fez (ESTF) and he was a member of the Transmission and Data Processing Laboratory (LTTI). In 1999, he received a second Doctorate in Electromagnetic Compatibility from Sidi Mohamed Ben Abdellah University (USMBA). Since 2009, he has been Vice-President of Research and Cooperation at the Sidi Mohamed Ben Abdellah University (USMBA) in Fez-Morocco until 2018. Currently, he is a Professor at the National School of Applied Sciences (ENSAF) and member of the LIASSE Laboratory at Sidi Mohamed Ben Abdellah University. He can be contacted at email: moulhime.elbekkali@usmba.ac.ma.

Catherine Algani 🆔 📇 SC ↻ born in 1963. Ph.D. in Electronics at the University Pierre and Marie Curie (Paris VI). University Professor at the National Conservatory of Arts and Crafts, CNAM-Paris. She is the responsible of the research team "communication systems" at ESYCOM laboratory. She can be contacted at email: catherine.algani@lecnam.net.